

# RPE65-Associated Retinopathies in the Italian Population: A Longitudinal Natural History Study

Francesco Testa,<sup>1</sup> Vittoria Murro,<sup>2</sup> Sabrina Signorini,<sup>3</sup> Leonardo Colombo,<sup>4</sup> Giancarlo Iarossi,<sup>5</sup> Francesco Parmeggiani,<sup>6,7</sup> Benedetto Falsini,<sup>8</sup> Anna Paola Salvetti,<sup>9</sup> Raffaella Brunetti-Pierri,<sup>1</sup> Giorgia Aprile,<sup>3</sup> Chiara Bertone,<sup>10</sup> Agnese Suppiej,<sup>11</sup> Francesco Romano,<sup>9</sup> Marianthi Karali,<sup>1,12</sup> Simone Donati,<sup>13</sup> Paolo Melillo,<sup>1</sup> Andrea Sodi,<sup>2</sup> Luciano Quaranta,<sup>10</sup> Luca Rossetti,<sup>4</sup> Luca Buzzonetti,<sup>5</sup> Marzio Chizzolini,<sup>7</sup> Stanislao Rizzo,<sup>8</sup> Giovanni Staurenghi,<sup>9</sup> Sandro Banfi,<sup>12,14</sup> Claudio Azzolini,<sup>13</sup> and Francesca Simonelli<sup>1</sup>

<sup>1</sup>Eye Clinic, Multidisciplinary Department of Medical, Surgical and Dental Sciences, University of Campania Luigi Vanvitelli, Naples, Italy

<sup>2</sup>Eye Clinic, Neuromuscular and Sense Organs Department, Careggi University Hospital, Florence, Italy

<sup>3</sup>Developmental Neuro-ophthalmology Unit, IRCCS Mondino Foundation, Pavia, Italy

<sup>4</sup>Eye Clinic, ASST Santi Paolo e Carlo Hospital, University of Milan, Milan, Italy

<sup>5</sup>Department of Ophthalmology, Bambino Gesù IRCCS Children's Hospital, Rome, Italy

<sup>6</sup>Department of Translational Medicine and for Romagna, University of Ferrara, Ferrara, Italy

<sup>7</sup>ERN-EYE Network–Center for Retinitis Pigmentosa of Veneto Region, Camposampiero Hospital, Padova, Italy

<sup>8</sup>Institute of Ophthalmology, Università Cattolica del Sacro Cuore, Rome, Italy

<sup>9</sup>Eye Clinic, Department of Biomedical and Clinical Science, Luigi Sacco Hospital, University of Milan, Milan, Italy

<sup>10</sup>Department of Surgical and Clinical, Diagnostic and Pediatric Sciences, Section of Ophthalmology, University of Pavia, IRCCS Fondazione Policlinico San Matteo, Pavia, Italy

<sup>11</sup>Department of Medical Sciences, University of Ferrara, Ferrara, Italy

<sup>12</sup>Telethon Institute of Genetics and Medicine, Pozzuoli, Italy

<sup>13</sup>Unit of Ophthalmology, Azienda Socio-Sanitaria Territoriale (ASST) Dei Sette Laghi, Department of Medicine and Surgery, University of Insubria, Varese, Italy

<sup>14</sup>Medical Genetics, Department of Precision Medicine, University of Campania Luigi Vanvitelli, Naples, Italy

Correspondence: Francesca Simonelli, Eye Clinic, Multidisciplinary Department of Medical, Surgical and Dental Sciences, Università degli Studi della Campania "Luigi Vanvitelli", via Pansini 5, Naples 80131, Italy; francesca.simonelli@unicampania.it.

FT, VM, SS, LC, GI, FP, BF, and APS contributed equally to the current study.

**Received:** August 25, 2021

**Accepted:** January 2, 2022

**Published:** February 7, 2022

Citation: Testa F, Murro V, Signorini S, et al. RPE65-associated retinopathies in the Italian population: A longitudinal natural history study. *Invest Ophthalmol Vis Sci.* 2022;63(2):13. <https://doi.org/10.1167/iovs.63.2.13>

**PURPOSE.** To investigate the course of inherited retinal degenerations (IRD) due to mutations in the *RPE65* gene.

**METHODS.** This longitudinal multicentric retrospective chart-review study was designed to collect best corrected visual acuity (BCVA), Goldman visual field, optical coherence tomography (OCT), and electroretinography (ERG) measurements. The data, including imaging, were collected using an electronic clinical research form and were reviewed at a single center to improve consistency.

**RESULTS.** From an overall cohort of 60 Italian patients with *RPE65*-associated IRD, 43 patients (mean age, 27.8 ± 19.7 years) were included and showed a mean BCVA of 2.0 ± 1.0 logMAR. Time-to-event analysis revealed a median age of 33.8 years and 41.4 years to reach low vision and blindness based on BCVA, respectively. ERG (available for 34 patients) showed undetectable responses in most patients (26; 76.5%). OCT (available for 31 patients) revealed epiretinal membranes in five patients (16.1%). Central foveal thickness significantly decreased with age at a mean annual rate of −0.6%/y ( $P = 0.044$ ). We identified 43 different variants in the *RPE65* gene in the entire cohort. Nine variants were novel. Finally, to assess genotype-phenotype correlations, patients were stratified according to the number of *RPE65* loss-of-function (LoF) alleles. Patients without LoF variants showed significantly ( $P < 0.05$ ) better BCVA compared to patients with one or two LoF alleles.

**CONCLUSIONS.** We described the natural course of *RPE65*-associated IRD in an Italian cohort showing for the first time a specific genotype-phenotype association. Our findings can contribute to a better management of *RPE65*-associated IRD patients.

**Keywords:** *RPE65* gene, Leber Congenital Amaurosis, Early-Onset Severe Retinal Dystrophy, genotype-phenotype correlation



The *RPE65* gene encodes a 65 kD retinoid isomerase expressed in the retinal pigment epithelium (RPE). This protein is a key component of the retinoid visual cycle because it converts all-trans-retinyl ester to 11-cis-retinol. When RPE65 is defective or absent, the 11-cis-retinal is depleted, which causes photoreceptor dysfunction.<sup>1</sup>

Biallelic *RPE65* variants were initially reported as the cause of Leber congenital amaurosis (LCA). This disease was first described by Theodore Leber in 1869 and is the most severe form of inherited retinal degenerations (IRD). LCA is characterized by total blindness or severely impaired vision at birth or within the first few months of life, normal fundus, nystagmus, poor pupil responses, and nonrecordable electroretinography (ERG).<sup>2</sup> LCA overlaps clinically and genetically with early-onset severe retinal dystrophy (EOSRD), which includes milder phenotypes.<sup>3</sup> The onset of EOSRD occurs between early childhood and five years of age. EOSRD patients usually preserve a better residual visual function (with minimal ERG signals) compared to LCA patients.<sup>4</sup> So far, LCA and EOSRD have been associated with disease-causing variants in 26 genes.<sup>3</sup> It has been reported that some genes are more likely to be associated with LCA, whereas variants in other genes, among which *RPE65*,<sup>5</sup> are more frequently encountered in EOSRD cases. *RPE65*-associated LCA/EOSRD accounts for approximately 5% to 10% of all IRD cases.<sup>6,7</sup> Moreover, variants in the *RPE65* gene have also been associated with a milder phenotype, namely fundus albipunctatus, with few cases described in literature.<sup>8–10</sup>

Given that the U.S. Food and Drug Administration and the European Medical Agency have approved a gene therapy for the treatment of patients with confirmed biallelic *RPE65* mutations, it is currently important to determine the natural history of *RPE65*-associated IRDs, also to compare the disease progression after treatment with the natural course of the retinal degeneration. Actually, *RPE65*-associated IRD has become one of the most studied forms of retinal degeneration, with several previous reports describing cases of *RPE65* patients,<sup>5,11–26</sup> also within cohorts of genetically heterogeneous patients with the same clinical diagnosis.<sup>27–41</sup> Recently, some studies reported data from large cohorts of *RPE65* patients. Specifically, Chung et al.<sup>42</sup> characterized 70 *RPE65* patients from six countries, whereas Pierrache et al.<sup>43</sup> analyzed a cohort of 45 Dutch patients. Finally, a cohort of 20 patients of Chinese origin was investigated.<sup>44</sup> However, all of these studies did not reveal any relevant genotype-phenotype correlation,<sup>42–44</sup> with the exception of the association of missense variants with fundus albipunctatus in a Chinese population.<sup>44</sup> Therefore information on the clinical course and its determinants (e.g., the *RPE65* genotype and genetic modifiers) from large cohorts is still needed.

To improve our understanding of the incidence and disease patterns of *RPE65*-associated IRDs, a large number of patients must be evaluated, using information technology (IT) systems. To date, several medical IT projects involving various medical specialties (e-health studies) have already given excellent results.<sup>45–47</sup> For these reasons, the Center for Rare Ocular Diseases of the University of Campania “Luigi Vanvitelli” (Naples, Italy) designed an e-health study involving nine Italian referral centers to carry out a quantitative analysis of clinical parameters in patients with IRDs caused by mutations in *RPE65*. Our multicentric study aimed to investigate the natural history of the *RPE65*-associated IRD and to seek genotype-phenotype correlations.

## METHODS

The study was conducted in accordance with the guidelines of the Declaration of Helsinki and subsequent revisions, and with the authorization of the Ethics Committees of the Coordinating (University of Campania “Luigi Vanvitelli”, Naples) and participating centers (Ospedale di Camposampiero, ULSS6 Euganea di Padova; AOU Careggi, Firenze; Ospedale San Paolo, Milano; Ospedale Sacco, Milano; Centro di Neuroftalmologia dell’età evolutiva, IRCCS Fondazione Istituto Neurologico Nazionale C. Mondino, Pavia; Policlinico di Pavia, Pavia; Policlinico Gemelli di Roma, Roma; Ospedale Bambino Gesù di Roma, Roma). The study has been registered on ClinicalTrials.gov (identifier: NCT04525261).

The study design, which was based on a retrospective chart review, was meant to allow a longitudinal comparison of patient care in different sites by using a dedicated e-health network platform. The primary goal of the study was to assess the structure and function of the retina in patients with IRDs caused by biallelic mutations in *RPE65* based on assessments of best corrected visual acuity (BCVA), visual field (VF), and optical coherence tomography (OCT).

Male and female subjects of any ethnicity were eligible for participation in this study, provided they could meet the following criteria:

1. Written informed consent (or parental permission and subject assent) to adhere to the protocol.
2. Subjects diagnosed with EOSRD or LCA.
3. Molecular diagnosis revealing biallelic variants (homozygotes or compound heterozygotes) in the *RPE65* gene.
4. Subjects aged three years old or older.
5. A minimum of two visits with ophthalmic assessment that spans a follow-up period of at least one year (for longitudinal analysis).

A subject was excluded from the study if he/she was unable or unwilling to meet the study requirements or had received gene therapy during the time-frame of the retrospective study.

The participating centers were selected on the basis of a standardized questionnaire that was distributed at the national level to collect information on eye clinics with know-how and expertise on the management of IRD patients.

The collected data included demographics (i.e., age and gender), self-reported age of onset of ocular symptoms (determined by the age at which patients or their parents first noticed nystagmus or visual abnormalities), ocular, medical, and surgical history, genetic and clinical diagnosis, BCVA, Goldman VF, OCT, ERG, and fundus imaging.

Protected health information was redacted before data collection in the ad hoc electronic clinical research form (eCRF). A dedicated database collecting data from various Italian centers with approved eCRF was designed in Naples (Italy) and finalized with the support of all collaborating Centers. All eCRFs were inserted and stored in the database with a special software. The system adopted was provided by Eumeda (Milan, Italy), which has long-standing experience in the development of medical software platforms. The system was stored in a protected data warehouse (Aruba Business srl, Ferrara, Italy) to ensure data security and uninterrupted availability. The same platform has been successfully used for other clinical trials.<sup>48–53</sup> This dedicated software enabled efficient and immediate data visualization and

quick data entry. The main developments in the software were application software for both computer and mobile device such as Tablets or Smartphones, successive multiple masks for first data entry and updating during follow-up, possibility to compare images taken during follow-up, pop-up windows to assist physicians and to ensure correct data entry, and data extraction for statistical purposes.

To avoid bias and improve consistency, criteria review and data entry for all charts, including imaging when available, were performed by investigators at the Coordinating Centre (F.T. and R.B.P. independently reviewed, and F.S. adjudicated in case of disagreement).

The clinical diagnosis was reviewed according to the following diagnostic criteria. A diagnosis of LCA was based on the presence of a severe visual impairment from birth (or from the first months of life), roving eye movements or nystagmus, poor pupillary light responses, oculo-digital sign (poking, rubbing, or pressing of the eyes), and undetectable or severely abnormal full-field ERG.<sup>3</sup> On the other hand, EOSRD was characterized by a later onset of visual impairment (typically after infancy, but before the age of five years), with variably preserved visual acuity and minimally preserved full-field ERG.<sup>3</sup>

The assessment of BCVA was performed either using a LEA symbol chart for children or the Tumbling E and EDTRS chart for adults. All assessments were converted to logarithm of the minimum angle of resolution (logMAR) unit for standardization purposes. Using the scale adapted from Holladay,<sup>54</sup> off-chart measurements were converted as follows: a value of 2.7 was assigned for hand motion, 2.8 for light perception, and 2.9 for no light perception. Moreover, BCVA were analyzed to evaluate low vision (i.e.,  $20/400 \leq$  BCVA in the better-seeing eye  $< 20/60$ ) or blindness (i.e., BCVA in the better-seeing eye  $< 20/400$ ) in accordance with the World Health Organization (WHO) criteria.

VF assessments were collected over time at different ages using manual Goldmann Kinetic perimetry and were analyzed to evaluate low vision (i.e., central VF diameter of the V4e target smaller than  $20^\circ$  but equal to or larger than  $10^\circ$  in the better-seeing eye) or blindness (central VF diameter of the V4e target smaller than  $10^\circ$  in the better-seeing eye) in accordance with the WHO criteria.

Full-field ERG was performed according to International Society for Clinical Electrophysiology protocol.<sup>55</sup>

Spectral-domain OCT was acquired using equipment from three different manufacturers (Carl Zeiss Meditec, Jena, Germany; Topcon Corporation, Optical Company, Tokyo, Japan; and Heidelberg Engineering GmbH, Heidelberg, Germany). OCT scans were carefully reviewed by two ophthalmologists with experience in the field of multimodal retinal imaging (A.P.S. and F.R.) for the following characteristics: presence of epiretinal membrane, thinning of the outer nuclear layer, disruption of the external limiting membrane, disruption of the ellipsoid zone in subfoveal and extrafoveal areas, atrophy of the RPE layer involving the fovea. The mean values provided by these two graders were considered for quantitative measurements, whereas a third senior grader (G.S.) was consulted to confirm the collected measures or in case of discordant qualitative findings. In addition, central foveal thickness (CFT), that is, the average thickness in the central subfield (circle with diameter of 1 mm) of the ETDRS grid, was analyzed. In particular, to analyze data obtained using devices of different manufacturers (i.e., Cirrus HD-OCT, Carl Zeiss Meditec; vs. Spectralis HRA+OCT, Heidelberg Engineering GmbH), CFT were

normalized against normative data reported in a previous study comparing values obtained with the two machines<sup>56</sup> (i.e.,  $258 \pm 21 \mu\text{m}$  for Cirrus HD-OCT vs.  $258 \pm 21 \mu\text{m}$  for Spectralis HRA+OCT). Given the low number of patients, CFT measurements provided by Topcon equipment were not included in the analysis.

## Statistics

Continuous variables are reported as mean  $\pm$  standard deviation, and categorical variables are reported as counts (frequency). The natural history of the disease was assessed with previously described methods in IRDs.<sup>57,58</sup> The annual progression rate of each endpoint was estimated by means of regression models for the analysis of longitudinal data, as appropriate. In particular, the generalized estimating equation was applied because this method can address both the intereye correlation (i.e., between the eyes of the same subject at a given visit) and the longitudinal correlation (i.e., among values of the same eye followed over time) by adopting an appropriate covariance structure, as previously described.<sup>59</sup> Because longitudinal data were not available for all testing parameters in all subjects and the duration of follow-up varied, the primary assessments were analyzed also using age as a proxy for time, so that all available individual data points could be included in the analysis. Furthermore, a Kaplan-Meier time-to-event analysis was performed to show the time to low vision and blindness based on BCVA or VF. Finally, Cohen's kappa coefficient ( $\kappa$ , range) was calculated to assess the agreement between the two independent graders for the qualitative OCT variables.  $P$  values  $< 0.05$  were considered statistically significant.

## RESULTS

### Clinical Characterization of the Cohort of RPE65 Patients

A total of 60 Italian patients from 56 families harboring disease-causing variants in the *RPE65* gene were screened for inclusion in the study. Seventeen patients were excluded for the following reasons: experimental treatment during the retrospective follow-up period (eight patients); no available clinical data (six patients); clinical diagnosis of fundus albipunctatus (two patients); age younger than three years (one patient). Therefore 43 patients (mean age,  $27.8 \pm 19.7$  years) with a clinical diagnosis of LCA (18/43 [41.9%]) or EOSRD (25/43 [58.1%]) harboring disease-causing mutations in the *RPE65* gene were further analyzed.

The main clinical findings of the included patients at the study baseline visits are summarized in Table 1. The self-reported age at onset of the first symptoms was  $2.2 \pm 2.1$  years (median: two years). The most frequent symptoms, mainly reported at birth or infancy, were low visual acuity ( $n = 32$  [74.4%]) and night blindness ( $n = 28$  [65.1%]). Moreover, more than half of the patients presented nystagmus (24/43 [55.8%]). Other frequently reported symptoms were photophobia ( $n = 20$  [46.5%]) and visual field loss ( $n = 18$  [41.9%]), whereas photopsia was referred by three patients (7.0%). Finally, only three patients (7.0%) showed the oculodigital sign.

Regarding the fundus evaluation, the most frequent findings were salt-and-pepper retinal dystrophy (i.e., RPE dystrophy with fine pigment clumping and dispersion) and RP fundus appearance, observed in 20 (46.5%) and 19 patients

**TABLE 1.** Main Clinical Findings of the Patients at the Study Baseline Visit Included in the Study Cohort

ID	Diagnosis	Age	Nystagmus	Fundus Evaluation	BCVA RE	BCVA LE	Electroretinogram
P1	EOSRD	4	No	Salt-and-pepper dystrophy	20/60	20/60	Reduced
P2	LCA	42	Yes	Salt-and-pepper dystrophy	LP	LP	Undetectable
P3	EOSRD	47	Yes	RP fundus appearance	HM	HM	Undetectable
P4	LCA	34	Yes	RP fundus appearance	20/600	20/1200	Undetectable
P5	LCA	32	Yes	Salt-and-pepper dystrophy	LP	LP	Undetectable
P6	EOSRD	46	Yes	RP fundus appearance	HM	HM	Undetectable
P7	EOSRD	24	Yes	Salt-and-pepper dystrophy	LP	LP	Undetectable
P8	LCA	33	Yes	RP fundus appearance	LP	LP	Undetectable
P9	EOSRD	56	No	RP fundus appearance	LP	LP	n.a.
P10	LCA	64	No	RP fundus appearance	LP	LP	Undetectable
P11	LCA	3	Yes	Normal	20/1200	20/1200	Reduced
P12	LCA	16	Yes	Salt-and-pepper dystrophy	20/2400	20/2400	n.a.
P13	EOSRD	68	No	RP fundus appearance	20/100	20/200	Undetectable
P14	EOSRD	41	Yes	RP fundus appearance	HM	HM	n.a.
P15	EOSRD	28	No	Salt-and-pepper dystrophy	20/20	20/25	Reduced
P16	EOSRD	24	No	RP fundus appearance	20/200	20/60	Undetectable
P17	EOSRD	44	Yes	RP fundus appearance	20/400	20/400	Undetectable
P18	EOSRD	13	No	RP fundus appearance	20/100	20/100	Undetectable
P19	LCA	43	No	RP fundus appearance	LP	LP	Undetectable
P20	EOSRD	4	No	Salt-and-pepper dystrophy	20/50	20/50	Undetectable
P21	EOSRD	39	No	RP fundus appearance	LP	LP	Undetectable
P22	LCA	5	Yes	RP fundus appearance	20/2400	20/2400	n.a.
P23	EOSRD	32	Yes	Salt-and-pepper dystrophy	HM	HM	Undetectable
P24	LCA	6	No	Salt-and-pepper dystrophy	20/100	20/100	Undetectable
P25	LCA	8	Yes	Salt-and-pepper dystrophy	20/400	20/400	Undetectable
P26	EOSRD	6	No	Salt-and-pepper dystrophy	20/100	20/100	Undetectable
P27	LCA	2	Yes	Normal	LP	LP	Reduced
P28	LCA	0	No	Normal	LP	LP	Reduced
P29	EOSRD	12	Yes	Salt-and-pepper dystrophy	20/100	20/200	Undetectable
P30	EOSRD	48	No	RP fundus appearance	HM	HM	n.a.
P31	EOSRD	6	No	Salt-and-pepper dystrophy	20/30	20/25	Markedly reduced
P32	EOSRD	34	Yes	RP fundus appearance	20/1200	20/1200	n.a.
P33	EOSRD	39	No	RP fundus appearance	20/25	20/25	n.a.
P34	LCA	48	No	Salt-and-pepper dystrophy	HM	HM	Undetectable
P35	EOSRD	25	Yes	Salt-and-pepper dystrophy	HM	HM	Undetectable
P36	LCA	36	Yes	Salt-and-pepper dystrophy	LP	HM	Undetectable
P37	EOSRD	22	Yes	RP fundus appearance	LP	HM	Undetectable
P38	LCA	18	No	Salt-and-pepper dystrophy	HM	HM	Undetectable
P39	EOSRD	61	Yes	RP fundus appearance	HM	HM	n.a.
P40	LCA	7	Yes	Normal	LP	LP	Markedly reduced
P41	LCA	11	Yes	Salt-and-pepper dystrophy	LP	LP	Markedly reduced
P42	EOSRD	60	No	Salt-and-pepper dystrophy	LP	LP	n.a.
P43	EOSRD	7	Yes	Salt-and-pepper dystrophy	20/60	20/100	Undetectable

RE, right eye; LE, left eye; HM, hand motion; LP, light perception; n.a., not available.

(44.2%), respectively. In four patients (9.3%) fundus abnormalities were not noted at the first visit. Patients with an RP fundus appearance were significantly older ( $42.6 \pm 14.6$  years;  $P < 0.001$ ) than those presenting a salt-and-pepper retinal dystrophy ( $18.3 \pm 15.1$  years) and normal fundus ( $5.4 \pm 4.5$  years). Overall, we did not observe any significant changes in the fundus appearance over the follow-up period.

In the study cohort, the mean BCVA was  $1.96 \pm 1.02$  logMAR in right eyes and  $1.97 \pm 1.00$  logMAR in left eyes. Blindness (i.e.,  $BCVA < 20/400$ ) was observed in the majority of patients (29 [67.4%]), whereas low vision (i.e.,  $20/400 \leq BCVA < 20/60$ ) was observed in seven patients (16.3%) and the remaining patients (7 [16.3%]) had a BCVA of 20/60 or better in at least one eye (Fig. 1A). The analysis of inter-eye asymmetry values revealed a very low asymmetry in

terms of BCVA (mean,  $0.05 \pm 0.11$ ; median = 0.00 logMAR) (Fig. 1B).

Longitudinal analysis of BCVA data collected in 35 patients over a mean follow-up period of  $5.0 \pm 4.5$  years (median, 4.6 years; range, 1–18 years) showed a nonsignificant decline ( $0.002 \pm 0.011$  logMAR/year;  $P = 0.835$ ). Changes in BCVA were observed only in 12 patients. Specifically, five adult patients (ID 4, 6, 17, 36, 37) and two children (ID 24, 31) showed a worsening of BCVA, whereas five pediatric patients (ID 1, 11, 27, 28, 43) showed some degree of improvement of their BCVA early in the disease course. Among these five pediatric patients, three had nystagmus (ID 11, 27, 43). Time-to-event analysis performed on BCVA data ( $n = 35$ ; mean follow-up period,  $5.0 \pm 4.5$  years; median, 4.6 years; range, 1–18 years) revealed a median age of 33.8 years and 41.4 years to reach low vision and blind-

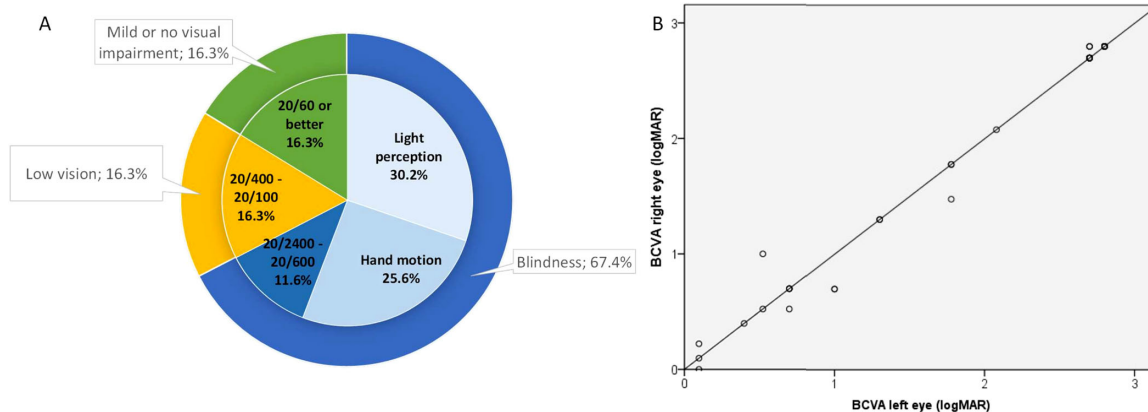


**FIGURE 1.** (A) Pie chart of BCVA measurements of the best-seeing eye of the 43 *RPE65* patients at the study baseline. (B) Comparison of BCVA measurement between both eyes measured in the 43 *RPE65* patients at the study baseline.

ness, respectively. Time-to-event analysis showed that the *RPE65* patients who underwent VF testing ( $n = 27$ ; mean follow-up period:  $5.8 \pm 4.7$  years; median, 4.8 years; range, 1–18 years) reached low vision at a mean age of 36.3 years and blindness at a mean age of 41.4 years.

The majority of patients ( $n = 28$  [65.1%]) had clear lens in both eyes, whereas lens opacities were observed in 11 patients (25.6%), and four patients (9.5%) were pseudophakic. As expected, patients with clear lens were younger than patients with lens opacities ( $18.3 \pm 15.3$  years vs.  $45.7 \pm 13.6$  years;  $P < 0.001$ ). The lens status did not significantly ( $P > 0.05$ ) affect BCVA in the age-adjusted models.

ERG examinations, performed in 34 patients, showed undetectable scotopic and photopic responses in 26 patients (76.5%), undetectable scotopic and reduced photopic responses in three patients (8.8%), and reduced scotopic and photopic responses in five (14.7%). The patients with detectable scotopic responses were younger ( $7.7 \pm 11.7$  years vs.  $26.9 \pm 18.7$  years;  $P = 0.034$ ) and showed a better BCVA ( $1.6 \pm 1.3$  logMAR vs.  $1.9 \pm 1.0$  logMAR;  $P = 0.544$ ).

Thirty-one patients underwent OCT scans acquired with Spectralis OCT ( $n = 12$ ), Cirrus HD-OCT ( $n = 13$ ), and Topcon equipment ( $n = 6$ ). Cystoid macular edemas, macular holes, or vitreomacular traction were not observed, whereas seven eyes of five patients (16.1%) showed epiretinal membranes. The manual review of Spectralis OCT scans showed that the majority of eyes disclosed thinning of the outer nuclear layer (19 [79%]), whereas the external limiting membrane appeared disrupted in 42% of the cases. The ellipsoid zone was more frequently altered in extrafoveal areas (16 eyes [67%]) than under the fovea (13 [54%]), and a minority of eyes had signs of RPE atrophy (8 [33%]) (Fig. 2). The inter-rater agreement for the analyzed measures was considered excellent ( $\kappa = 0.89$ ; range: 0.75–1.00) (Table 2). The mean CFT was  $172.3 \pm 42.6$   $\mu\text{m}$  in the right eyes and  $174.9 \pm 35.2$   $\mu\text{m}$  in the left eyes. Furthermore, OCT scans acquired with the Cirrus HD-OCT showed a mean CFT of  $166.5 \pm 61.0$   $\mu\text{m}$  in the right eyes and  $172.0 \pm 45.2$   $\mu\text{m}$  in the left eyes. To combine for further analyses the OCT measurements obtained with both equipment (i.e., Spectralis vs. Cirrus HD-OCT), CFT values were first normalized against normative data. The cross-sectional analysis (25 patients) showed a significant decrease of the normalized CFT with age at a mean exponential rate of  $-0.6\%$  per year (95% confidence interval,  $-1.2\%$  to  $0.0002\%$ ;  $P = 0.044$ ). The normal-

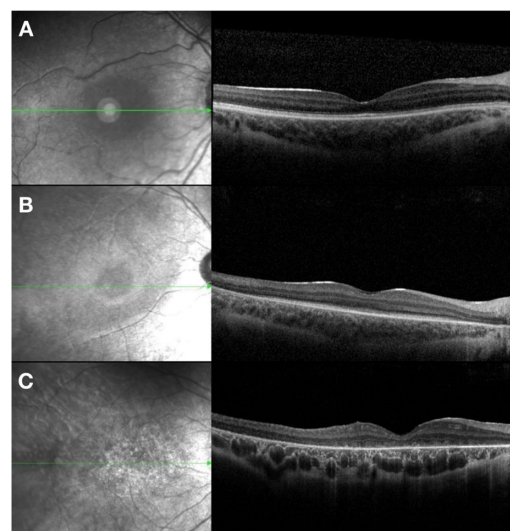


**FIGURE 2.** Examples of qualitative analysis of OCT scans in selected patients: (A) an initial thinning of the outer nuclear layer (ONL), an intact external limiting membrane (ELM) and initial parafoveal defects of the ellipsoid zone (EZ); (B) thinning of the ONL, preservation of the ELM and disruption of the EZ, whereas the RPE layer is still preserved; (C) final stage of retinal degeneration with complete atrophy of the ELM, EZ and RPE layers; the outer plexiform layer can instead be observed as a rarefied hyperreflective band lying above the ONL.

ized CFT also correlated negatively with BCVA, expressed in logMAR ( $\rho = -0.283$ ;  $P$  value = 0.048). Finally, the longitudinal analysis ( $n = 20$ ; mean follow-up period,  $3.9 \pm 2.9$  years; median, 3.0 years; range, 1–10 years) did not show a significant decline (exponential rate,  $-0.2\%$ /year; 95% confidence interval,  $-3.0\%$  to  $2.7\%$ ;  $P = 0.9$ ).

### Molecular Characterization of the *RPE65* Cohort and Genotype-Phenotype Correlation Analysis

Less than half of the patients ( $n = 24$ ; 40%) were homozygous for the identified variants, whereas the remaining 60% ( $n = 36$ ) were compound heterozygotes. In the cohort of 60 patients (that comprised also cases excluded from the clinical characterization), we identified a total of 43 different

**TABLE 2.** Inter-Rater Agreement for the Qualitative OCT Findings

	k Value
ERM presence	1.00
ONL thinning	0.75
ELM disruption	0.83
Foveal EZ disruption	0.83
Extrafoveal EZ disruption	0.81
RPE atrophy	1.00

ERM, epiretinal membrane; ONL, outer nuclear layer; ELM, external limiting membrane; EZ, ellipsoid zone; RPE, retinal pigment epithelium.

variants in the *RPE65* gene (Table 3; Fig. 3A), namely, seven frameshift variants, eight nonsense mutations, four splice-site variants, and 24 missense variants (Fig. 3B). The vast majority of variants (94%) were classified in Varsome<sup>60</sup> as “pathogenic” (n = 23; 54%) or “likely pathogenic” (n = 17; 40%) (Fig. 3C), according to the guidelines of the American College of Medical Genetics and Genomics (ACMG) and the Association for Molecular Pathology.<sup>61</sup> Only three missense variants (p.Arg85Cys, p.Thr149Asn, and p.Thr153Arg) were reported as variants of uncertain significance (VUS) (Fig. 3C). The latter VUS were predicted to be “disease causing” by MutationTaster (<http://www.mutationtaster.org/>) and were either absent from the Genome Aggregation Database (gnomAD; <http://gnomad.broadinstitute.org>) or had a minor allele frequency compatible with a probable pathogenic role.

In all three cases, the patients carrying these VUS were also heterozygous for a missense “likely pathogenic” variant (p.Pro371Leu, p.Phe336Ser, and p.Arg91Trp, respectively).

Nine of the identified variants were novel (Table 3). These variants were not previously reported in reference databases (e.g., human gene mutation database, LOVD, and ClinVar) or in literature. For the novel missense variants, in silico pathogenicity predictions, allele frequency in control population databases and pathogenicity interpretation according to the ACMG recommendations<sup>61</sup> (either by manual assessment or based on the Varsome annotation) are reported in Table 4.

To assess whether the patients’ genotypes correlated with disease severity, we stratified the included sample of 43 patients according to the number of *RPE65* loss-of-function (LoF) alleles identified in each subject. We considered frameshifts and nonsense variants as bona fide LoF mutations, whereas missense changes were classified as non-LoF. In this classification, splice-site variants were not considered as LoF because their impact on the transcript and protein cannot be reliably predicted. By applying these criteria, we divided our cohort into three genotypic categories: group A comprised 21 patients who did not harbor any LoF variant (e.g., they carried only missense variants); group B comprised 13 compound heterozygous patients for an LoF mutation and a non-LoF variant; group C consisted of nine patients who carried biallelic LoF variants. The mean age of patients was not significantly different for the three genotypic groups (group A: 33.6 ± 18.6 years; group B:

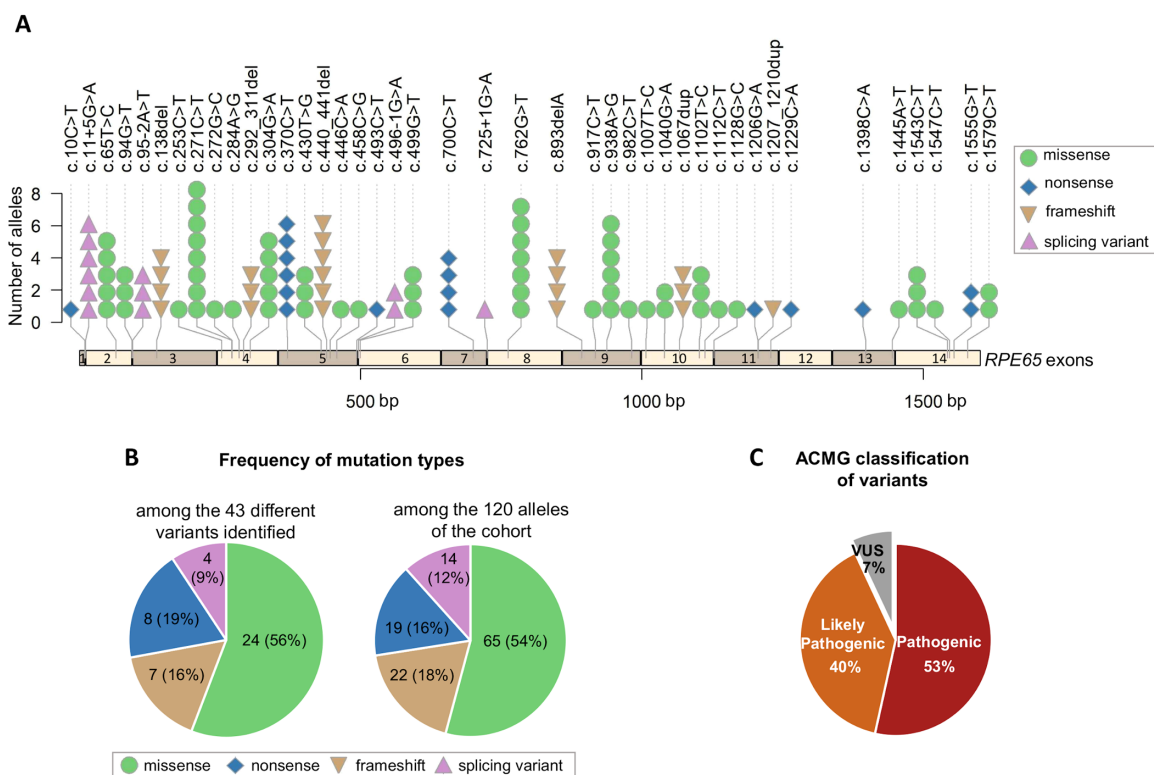


**FIGURE 3.** Genetic variants detected in *RPE65* in the study cohort. (A) Schematic drawing of the *RPE65* exons showing the position of the variants identified and their frequency among index cases. The nucleotide change and variant position is reported on the top. The colored symbol shape indicates the mutation type (specified in the legend box). (B) Pie charts showing the relevant representation of the different mutation types among the 43 different variants identified (left panel) and among the 120 alleles of the entire cohort (right panel). (C) Pie chart showing the classification of the identified sequence variants according to the ACMG guidelines using the Varsome automated variant classification.<sup>60</sup>

TABLE 3. Genotypes of the Molecularly Confirmed RPE65 Patients of the Italian Cohort

Patient ID	Included	Variant 1			Variant 2			Group
		DNA Change	Protein Change	Reference	DNA Change	Protein Change	Reference	
P1	Yes	c.95-2A>T	p.?	33	c.1040G>A	p.Arg347His	34	A
P2	Yes	c.938A>G	p.His313Arg	27	c.938A>G	p.His313Arg	27	A
P3	Yes	c.11+5G>A	p.?	74	c.271C>T	p.Arg91Trp	62	A
P4	Yes	c.725+1G>A	p.?	This study	c.271C>T	p.Arg91Trp	62	A
P5	Yes	c.271C>T	p.Arg91Trp	62	c.271C>T	p.Arg91Trp	62	A
P6	Yes	c.94G>T	p.Gly32Cys	65	c.917C>T	p.Thr306Ile	35	A
P7	Yes	c.304G>A	p.Glu102Lys	62	c.304G>A	p.Glu102Lys	62	A
P8	Yes	c.272G>C	p.Arg91Pro	27	c.430T>G	p.Tyr144Asp	23	A
P9, P10	Yes	c.11+5G>A	p.?	74	c.11+5G>A	p.?	52	A
P11	Yes	c.762G>T	p.Glu254Asp	77	c.762G>T	p.Glu254Asp	77	A
P12	Yes	c.95-2A>T	p.?	33	c.95-2A>T	p.?	33	A
P13	Yes	c.65T>C	p.Leu22Pro	25	c.65T>C	p.Leu22Pro	25	A
P14	Yes	c.1579C>T	p.His527Tyr	This study	c.1579C>T	p.His527Tyr	This study	A
P15	Yes	c.1112C>T	p.Pro371Leu	36	c.253C>T	p.Arg85Cys	37	A
P16	Yes	c.65T>C	p.Leu22Pro	25	c.1128G>C	p.Lys376Asn	This study	A
P17	Yes	c.430T>G	p.Tyr144Asp	23	c.430T>G	p.Tyr144Asp	23	A
P18	Yes	c.762G>T	p.Glu254Asp	77	c.762G>T	p.Glu254Asp	77	A
P19	Yes	c.271C>T	p.Arg91Trp	62	c.271C>T	p.Arg91Trp	62	A
P20	Yes	c.458C>G	p.Thr153Arg	This study	c.1007T>C	p.Phe336Ser	This study	A
P21	Yes	c.11+5G>A	p.?	14	c.284A>G	p.Glu95Gly	38	A
P22	Yes	c.370C>T	p.Arg124*	62	c.496-1G>A	p.?	78	B
P23	Yes	c.292_311del	p.Ile98Hisfs*26	64	c.938A>G	p.His313Arg	27	B
P24	Yes	c.65T>C	p.Leu22Pro	25	c.10C>T	p.Gln4*	This study	B
P25	Yes	c.11+5G>A	p.?	46	c.700C>T	p.Arg234*	24	B
P26	Yes	c.1543C>T	p.Arg515Trp	39	c.1555G>T	p.Glu519*	This study	B
P27, P28	Yes	c.1102T>C	p.Tyr368His	12	c.1229C>A	p.Ser410*	This study	B
P29	Yes	c.499G>T	p.Asp167Tyr	66	c.292_311del	p.Ile98Hisfs*26	64	B
P30	Yes	c.1543C>T	p.Arg515Trp	39	c.1067dup	p.Asn356Lysfs*9	29	B
P31	Yes	c.1067dup	p.Asn356Lysfs*9	74	c.1547C>T	p.Ala516Val	This study	B
P32	Yes	c.11+5G>A	p.?	74	c.493C>T	p.Gln165*	40	B
P33	Yes	c.1067dup	p.Asn356Lysfs*9	74	c.65T>C	p.Leu22Pro	25	B
P34	Yes	c.271C>T	p.Arg91Trp	62	c.440_441del	p.Thr147Argfs*9	27	B
P35	Yes	c.138del	p.Pro47Glnfs*47	64	c.138del	p.Pro47Glnfs*47	64	C
P36	Yes	c.893delA	p.Lys298Serfs*27	41	c.893delA	p.Lys298Serfs*27	41	C
P37	Yes	c.370C>T	p.Arg124*	62	c.370C>T	p.Arg124*	62	C
P38	Yes	c.438_439del	p.Thr147Argfs*9	79	c.438_439del	p.Thr147Argfs*9	79	C
P39	Yes	c.1398C>A	p.Tyr466*	26	c.1555G>T	p.Glu519*	This study	C
P40, P41	Yes	c.1207_1210dup	p.Glu404Alafs*4	62	c.1206G>A	p.Trp402*	78	C
P42	Yes	c.370C>T	p.Arg124*	62	c.700C>T	p.Arg234*	24	C
P43	Yes	c.893delA	p.Lys298Serfs*27	41	c.893delA	p.Lys298Serfs*27	41	C
P44	No	c.370C>T	p.Arg124*	62	c.496-1G>A	p.?	78	B
P45, P46	No	c.304G>A	p.Glu102Lys	62	c.304G>A	p.Glu102Lys	62	A
P47	No	c.762G>T	p.Glu254Asp	77	c.762G>T	p.Glu254Asp	77	A
P48	No	c.271C>T	p.Arg91Trp	62	c.446C>A	p.Thr149Asn	72	A
P49	No	c.499G>T	p.Asp167Tyr	66	c.938A>G	p.His313Arg	27	A
P50	No	c.938A>G	p.His313Arg	27	c.1102T>C	p.Tyr368His	12	A
P51	No	c.938A>G	p.His313Arg	27	c.1445A>T	p.Asp482Val	80	A
P52	No	c.700C>T	p.Arg234*	24	c.700C>T	p.Arg234*	24	C
P53	No	c.94G>T	p.Gly32Cys	65	c.94G>T	p.Gly32Cys	65	A
P54	No	c.370C>T	p.Arg124*	62	c.1543C>T	p.Arg515Trp	39	B
P55	No	c.292_311del	p.Ile98Hisfs*26	64	c.499G>T	p.Asp167Tyr	66	B
P56	No	c.304G>A	p.Glu102Lys	62	c.440_441del	p.Thr147Argfs*9	27	B
P57	No	c.138del	p.Pro47Glnfs*47	64	c.138del	p.Pro47Glnfs*47	64	C
P58	No	c.440_441del	p.Thr147Argfs*9	27	c.440_441del	p.Thr147Argfs*9	27	C
P59	No	c.1040G>A	p.Arg347His	34	c.1102T>C	p.Tyr368His	12	A
P60	No	c.982C>T	p.Leu328Phe	10	c.762G>T	p.Glu254Asp	77	A

18.7 ± 18.4 years; group C: 27.5 ± 21.0 years;  $P = 0.10$ ). The age-adjusted model on cross-sectional data ( $n = 43$ ) showed a significantly ( $P < 0.05$ ) better BCVA in group A and B compared to group C (Fig. 4). Moreover, time-to-event analysis based on longitudinal data available for 35

patients (mean follow-up period, 5.0 ± 4.5 years; median, 4.6 years; range, 1–18 years) indicated that group A patients reached low vision at significantly ( $P = 0.019$ ) older median age (41.5 years) than group B (11.5 years) and group C (25.4 years) (Fig. 5). Similarly, we observed that group C

**TABLE 4.** Pathogenicity Predictions for the Novel Missense *RPE65* Variants Detected in This Cohort

Nucleotide/ Protein Change	ACMG Classification		Computational Verdict of Pathogenicity (Acc. to VarSome <sup>e</sup> )	In Silico Pathogenicity Predictions			Allele Frequency
	Manually Assessed	In VarSome <sup>e</sup>		MutationTaster <sup>†</sup>	PolyPhen-2 <sup>‡</sup>	Cadd13 <sup>§</sup>	
c.458C>G/ p.Thr153Arg	Likely Pathogenic (PM2, PM5, PP2, PP3, PP4)	Uncertain Significance	Pathogenic (7 pathogenic vs. 5 benign predictions)	Disease causing (score: 71)	Benign (score: 0.006)	23.4	NR
c.1007T>C/ p.Phe336Ser	Uncertain significance (PM2, PP2, PP3, PP4)	Likely Pathogenic	Pathogenic (10 pathogenic vs. 2 benign predictions)	Disease causing (score: 155)	Prob. Damaging (score: 0.976)	24.5	NR
c.1128G>C <sup>  </sup> / p.Lys376Asn	Pathogenic (PVS1, PM2, PP2, PP3, PP4)	Pathogenic	Pathogenic (8 pathogenic vs. 5 benign predictions)	Disease causing (score: 94)	Benign (score: 0.156)	33	NR
c.1445A>T/ p.Asp482Val	Likely Pathogenic (PM2, PM3, PP2, PP3, PP4)	Likely Pathogenic	Pathogenic (11 pathogenic vs. 1 benign prediction)	Disease causing (score: 152)	Prob. Damaging (score: 0.970)	28.7	NR
c.1547C>T/ p.Ala516Val	Likely Pathogenic (PM2, PM3, PP2, PP3, PP4)	Likely Pathogenic	Pathogenic (11 pathogenic vs. 1 benign prediction)	Disease causing (score: 64)	Prob. Damaging (score: 0.995)	29.2	NR
c.1579C>T/ p.His527Tyr	Likely Pathogenic (PM1, PM2, PM5, PP2, PP3, PP4)	Likely Pathogenic	Pathogenic (11 pathogenic vs. 1 benign prediction)	Disease causing (score: 83)	Prob. Damaging (score: 1.000)	27.8	4.00e-6 (gnomAD) 8.27e-6 (ExAC)

NR, not reported in the Genome Aggregation Database (gnomAD), in the Exome Aggregation Consortium (ExAC) database and in the 1000 Genomes Project catalogue.

All nucleotide positions refer to the transcript NM\_000329.

<sup>e</sup><http://varsome.com/>.<sup>60</sup>

<sup>†</sup><http://www.mutationtaster.org/>.

<sup>‡</sup>Polymorphism Phenotyping v2; <http://genetics.bwh.harvard.edu/pph2/>.

<sup>§</sup>Combined Annotation-Dependent Depletion; <http://cadd.gs.washington.edu/>.

<sup>||</sup> Canonical splice site.

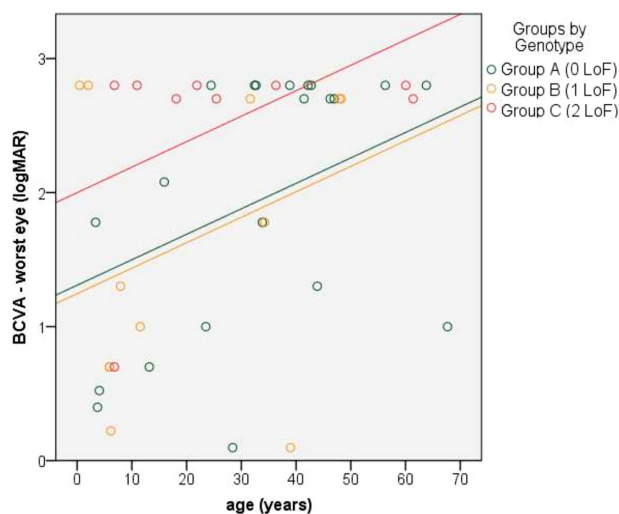


**FIGURE 4.** Comparison of BCVA measurements (best-seeing eye) at the study baseline in the 43 *RPE65* patients stratified according to the genotype. Patients harboring biallelic LoF variants (Group C, red circles) had a significantly worse BCVA compared to the other groups (Group B, compound heterozygotes for an LoF and a missense variant, yellow circles; Group A, biallelic missense variants, green circles).

patients reached blindness, as determined by either BCVA or VF tests, at a younger median age (BCVA, 25.4 years; VF, 25.4 years) than group A (BCVA, 42.2 years; VF, 42.7 years) and B (BCVA, 47.9 years; VF, 34.2 years), but these differences were not statistically significant ( $P > 0.05$ ). Finally, we observed the following trend, which did not achieve the statistically significant level ( $P > 0.05$ ): nystagmus was observed in the majority of group C patients (77.8%) and

only in about 50% of patients in group A and group B; all the group C patients (100%) showed an undetectable scotopic ERG whereas about 20% of patients in group A and B had detectable scotopic ERG; at the fundus evaluation, the majority of group B (7/13; 53.8%) and of group C (6/9; 66.7%) showed a salt-and-pepper dystrophy whereas the majority of group A patients (13/21; 68.4%) showed an RP fundus. No significant differences were observed in the age of onset ( $P = 0.714$ ) or in the normalized CFT ( $P = 0.831$ ).

## Discussion

We report the main findings of a retrospective longitudinal study that assessed the natural course of the disease in *RPE65*-associated IRDs in a large cohort of Italian subjects ( $n = 43$ ) from nine Italian Referral Centers with expertise in IRDs. Given the absence of a national epidemiological registry, this study represents the first attempt to assess the figures of *RPE65*-associated IRDs in Italy. The data available at the Coordinating Centre, which identified the highest number of patients, suggested that *RPE65* cases account for about 10% of the LCA/EOSRD in the Italian population (26 cases of approximately 250 LCA/EOSRD patients). This incidence is consistent with estimates from other cohorts with a reported range of 4% to 15%.<sup>62–66</sup>

The review of clinical diagnosis in the Italian cohort confirmed that *RPE65* mutations are associated with a common phenotype (e.g., severe rod dysfunction, detectable cone function, structural-functional dissociation, relative fovea sparing despite abnormal acuities, scarcity of pigmentary change in the early disease stage, whitish deposits, RP-like fundus appearance later in life)<sup>67–69</sup> with a spectrum of disease severity, that ranges from a mild form, clinically diagnosed as congenital stationary night blindness, to a severe one, diagnosed as LCA. Moreover, the



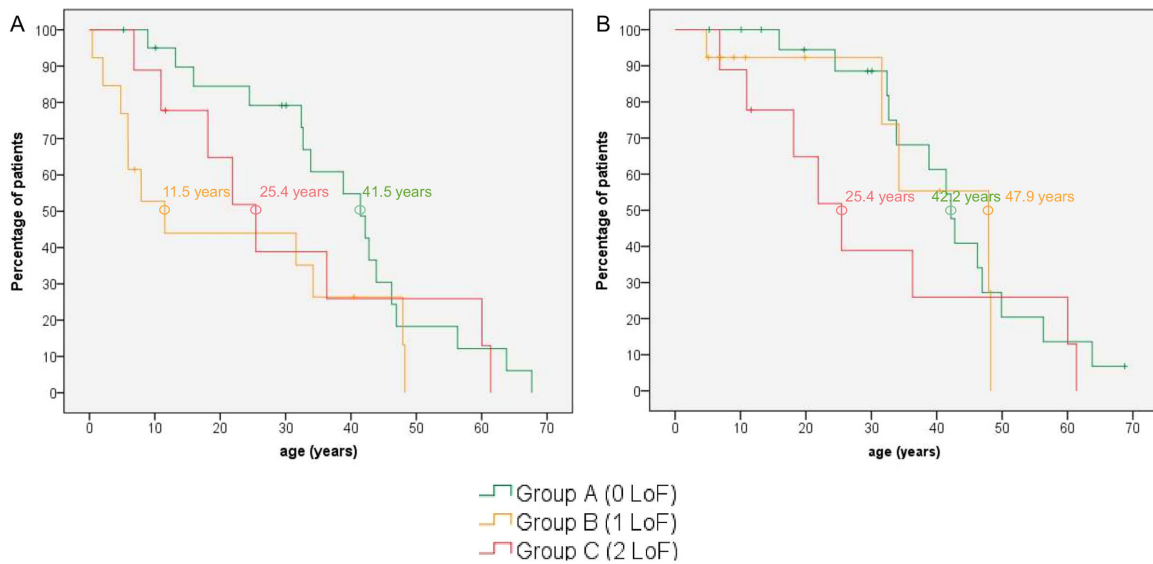


**FIGURE 5.** Time-to-event analysis for low vision, i.e.,  $20/400 \leq$  BCVA in the better-seeing eye  $< 20/60$ , (A) and blindness, i.e., BCVA in the better-seeing eye  $< 20/400$ , (B) based on longitudinal observations ( $n = 35$ ; mean follow-up period:  $5.0 \pm 4.5$  years; median, 4.6 years; range, 1–18 years) in the study sample stratified according to genotype.

majority of patients had an intermediate form termed as EOSRD, whereas fundus albipunctatus, a form of congenital stationary night blindness, was diagnosed only in two Italian patients who had a similar retinal phenotype to the cases previously described.<sup>8–10,44</sup> Differently from other studies,<sup>42,70</sup> we did not diagnose any case of cone-rod dystrophy.

With regard to visual function, we observed considerable variability in BCVA between patients, particularly in the first decades of life. Moreover, BCVA was better in our study sample compared to the two largest published cohorts<sup>42,43</sup> in which all patients over 40 years of age were blind according to the WHO criteria for visual acuity (i.e.,  $< 20/400$  in both eyes). Specifically, at the age of 41.4 years, only 50% of our patients were blind. Also, VF evaluation and ERG responses suggested a better preserved retinal function in our cohort compared to the one described by Pierrache et al.<sup>43</sup> The latter had a younger median age of low vision based on VF compared to our cases (i.e., third vs. fourth decade of life) and a lower percentage of detectable ERG responses compared to our cohort (i.e., 13.8% vs. 23.5%). Finally, we observed a transient improvement of BCVA in some pediatric subjects, which may be attributed to the maturation of their visual system and overall development (e.g., collaboration during evaluation session, attention span, better ability to perform symbol recognition test), as well as to improved functional vision after visual rehabilitation, as suggested by previous studies.<sup>42,63</sup>

Slit lamp and fundus evaluation revealed that structural abnormalities (e.g., lens opacity, retinal vessel attenuations, retinal pigments) also increase with age. In particular, as previously suggested,<sup>43</sup> signs of retinal degeneration, such as bone spicule pigmentation and RPE atrophy, become apparent only in the second decade of life or later.

Unlike BCVA and VF assessments, very few patients performed OCT measurements with the same equipment during the follow-up visits, limiting the analysis of the retinal layer changes. In this regard, it is often difficult to obtain good-quality scans in patients with poor visual function and

severe nystagmus. Nevertheless, the cross-sectional analysis of the pooled data obtained by Spectralis and HD-Cirrus OCTs showed a statistically significant effect of age on CFT, suggesting a progression of the retinal degeneration over decades. The available scans confirmed that retinal architecture in the macular region was mostly preserved during childhood with an excellent agreement between different observers. A markedly reduced CFT (i.e.,  $< 100 \mu\text{m}$ ), which precludes surgical treatment with Voretigene Neparvovec,<sup>71</sup> was observed in only six patients (19.3%) who were 35 years old or older. Therefore, although the treatment should be performed as early as possible to achieve the maximum benefit,<sup>72</sup> our data suggest that the intervention window for subretinal gene therapy may be extended also to the third decade of life.

Almost all patients (57 of 60) carried biallelic, high confidence “pathogenic” or “likely pathogenic” variants in *RPE65* (Fig. 3C). Only three subjects were compound heterozygotes for a variant of “uncertain significance” (VUS) and a (“likely”) pathogenic” variant. Given that these three patients have a phenotype that is highly specific for the *RPE65* disease and had performed a comprehensive molecular analysis that excluded the causative role of other genes, we strongly believe that these VUS likely represent bona fide pathogenic variants. In particular, the c.446C>A (p.Thr149Asn) variant is classified in the human gene mutation database as a likely pathological mutation.<sup>72</sup> Moreover, the c.253C>T (p.Arg85Cys) variant has a pathogenic computational verdict in Varsome,<sup>60</sup> considering the 12 pathogenic (vs. no benign) predictions from in silico tools. Finally, after a manual implementation of the ACMG criteria, the variant p.Thr153Arg was classified as “likely pathogenic” because a different substitution of the Thr153 residue (p.Thr153Ala) was previously reported as pathogenic (PM5)<sup>73</sup> (Table 4).

Of the 43 variants identified in this study, more than half were predicted to cause missense amino acid changes (Fig. 3B). This is consistent with the high prevalence of *RPE65* missense mutations in variant repositories (reviewed by Aoun et al.<sup>6</sup> and described in other cohorts<sup>43,44</sup>). Two

of the identified missense variants (c.94G>T; p.Gly32Cys and c.1445A>T; p.Asp482Val) involved canonical splice sites and were likely to interfere with normal splicing. The most frequently detected variations in the entire cohort (n = 8) were the splicing variant c.11+5G>A<sup>74</sup> and the missense variant c.271C>T (p.Arg91Trp)<sup>62</sup> (Table 3). Although the latter was previously described as a hypomorphic allele, associated with low but substantial levels of both RPE65 and 11-cis-retinal in a murine model,<sup>75</sup> we observed a severe phenotype in two unrelated patients (P5 and P19) homozygous for this variant, who had a clinical diagnosis of LCA, nystagmus, keratoconus, light perception, and nondetectable ERG at the study baseline (at 32 and 43 years, respectively). Their clinical presentation was quite similar to the three siblings, homozygous for the same variant, recently described by Magliyah et al.,<sup>22</sup> who reported nystagmus and nondetectable ERG in all the siblings and light perception in two patients (at the age of 32 and 36 years), whereas the third cases had a slightly better visual acuity (20/100 at 34 years). Finally, the two patients diagnosed with fundus albipunctatus (P59, P60) were compound heterozygotes for missense variants, one of which (c.982C>T) was previously reported in a patient with the same diagnosis.<sup>10</sup>

Differently from the Dutch cohort,<sup>43</sup> the three pairs of siblings in the Italian cohort did not show a relevant intrafamilial variability in terms of either visual function or retinal phenotype. Moreover, the analysis of interfamilial variability shows only a significant difference between the cases homozygous for the variant c.762G>T; p.Glu254Asp (i.e., patient 11 and patient 18), because the younger patient showed a more severe phenotype, classified as LCA with an earlier disease onset and a worse visual acuity compared to the older case, who received a clinical diagnosis of EOSRD.

Previous studies did not show any relevant genotype-phenotype correlation.<sup>42–44</sup> Conversely, we show a significant correlation between visual function and the number of LoF alleles. Specifically, we found that patients with no LoF variants (group A) had a better preserved visual acuity and ERG responses compared to those with two LoF alleles (group C). In particular, group A patients reached on average low vision about 15 years later than group C patients. Our results are in line with the findings observed on static full-field perimetry by Kumaran et al.,<sup>76</sup> who reported that subjects with at least one LoF variant showed greater progressive loss of retinal sensitivity in the second decade of life than those without. In addition, we observed that the absence of nystagmus and RP fundus are more frequent in group A patients (about 50% and 70%, respectively), whereas about 70% of group C patients presented salt-and-pepper dystrophy and nystagmus.

Our study has some limitations mainly related to its retrospective design. First, there are differences in the follow-up time and visit frequency among patients. Second, some examinations, particularly the OCT, could not be consistently performed across the cohort because of severe nystagmus and patient compliance. Moreover, the spectral domain OCT was not available in earlier visits. Finally, not all patients were willing to be re-examined in follow-up visits. That notwithstanding, given the rarity and the clinical features of the disease, the study design seems the most appropriate for this patient population, in line with previous studies.<sup>42,43</sup> In particular, the involvement of several centers is required because of the rarity of the disease, although this led to significant issues about quality of data and compar-

bility of findings observed with different equipment, particularly concerning OCT acquisition. To improve the quality of data, we implemented an ad hoc eCRF with capability to collect imaging and reviewed all data, including imaging, at a single center that acted as the reading center.

In conclusion, our data delineate the natural course of IRDs in a cohort with biallelic mutations in *RPE65*, confirming the spectrum of retinal phenotypes that range from LCA to fundus albipunctatus. We observed for the first time a relevant genotype-phenotype association, showing that patients who do not harbor any LoF variants have a better visual acuity, a better preserved ERG, and are more likely to show no nystagmus, and RP fundus. Our findings provide useful information to improve the clinical and therapeutic management of patients with *RPE65*-associated IRD.

### Acknowledgments

The authors thank the patient association Retina Italia Onlus, particularly, its President Assia Andrao, for the funding support and sponsorship of this natural history study. They are grateful to the European Reference Network dedicated to Rare Eye Diseases (ERN-EYE) for useful discussions.

Supported by Retina Italia Onlus.

Disclosure: **F. Testa**, None; **V. Murro**, None; **S. Signorini**, None; **L. Colombo**, None; **G. Iarossi**, None; **F. Parmeggiani**, None; **B. Falsini**, None; **A.P. Salvetti**, None; **R. Brunetti-Pierri**, None; **G. Aprile**, None; **C. Bertone**, None; **A. Suppiej**, None; **F. Romano**, None; **M. Karali**, None; **S. Donati**, None; **P. Melillo**, None; **A. Sodi**, None; **L. Quaranta**, None; **L. Rossetti**, None; **L. Buzzonetti**, None; **M. Chizzolini**, None; **S. Rizzo**, None; **G. Staurenghi**, None; **S. Banfi**, None; **C. Azzolini**, None; **F. Simonelli**, None

### References

- den Hollander AI, Roepman R, Koenekoop RK, Cremers FP. Leber congenital amaurosis: genes, proteins and disease mechanisms. *Prog Retin Eye Res.* 2008;27:391–419.
- Franceschetti A, Dieterle P. [Diagnostic and prognostic importance of the electroretinogram in tapetoretinal degeneration with reduction of the visual field and hemeralopia]. *Confin Neurol.* 1954;14:184–186.
- Kumaran N, Moore AT, Weleber RG, Michaelides M. Leber congenital amaurosis/early-onset severe retinal dystrophy: clinical features, molecular genetics and therapeutic interventions. *Br J Ophthalmol.* 2017;101:1147–1154.
- Kumaran N, Pennesi ME, Yang P, et al. Leber congenital amaurosis /early-onset severe retinal dystrophy overview. *GeneReviews [Internet].* 2018.
- Weleber RG, Michaelides M, Trzupek KM, Stover NB, Stone EM. The phenotype of Severe Early Childhood Onset Retinal Dystrophy (SECORD) from mutation of RPE65 and differentiation from Leber congenital amaurosis. *Invest Ophthalmol Vis Sci.* 2011;52:292–302.
- Aoun M, Passerini I, Chiurazzi P, et al. Inherited retinal diseases due to RPE65 variants: from genetic diagnostic management to therapy. *Int J Mol Sci.* 2021;22:7207.
- Kumaran N, Moore AT, Weleber RG, Michaelides M. Leber congenital amaurosis/early-onset severe retinal dystrophy: clinical features, molecular genetics and therapeutic interventions. *Br J Ophthalmol.* 2017;101:1147–1154.
- Schatz P, Preising M, Lorenz B, Sander B, Larsen M, Rosenberg T. Fundus albipunctatus associated with compound heterozygous mutations in RPE65. *Ophthalmology.* 2011;118:888–894.

9. Ramtohl P, Denis D. RPE65-mutation associated fundus albipunctatus with cone dystrophy. *Ophthalmol Retina*. 2019;3:535.
10. Yang G, Liu Z, Xie S, et al. Genetic and phenotypic characteristics of four Chinese families with fundus albipunctatus. *Sci Rep*. 2017;7:46285.
11. Felius J, Thompson DA, Khan NW, et al. Clinical course and visual function in a family with mutations in the RPE65 gene. *Arch Ophthalmol*. 2002;120:55–61.
12. Lorenz B, Gyurus P, Preising M, et al. Early-onset severe rod-cone dystrophy in young children with RPE65 mutations. *Invest Ophthalmol Vis Sci*. 2000;41:2735–2742.
13. Lorenz B, Poliakov E, Schambeck M, Friedburg C, Preising MN, Redmond TM. A comprehensive clinical and biochemical functional study of a novel RPE65 hypomorphic mutation. *Invest Ophthalmol Vis Sci*. 2008;49:5235–5242.
14. Lorenz B, Wabbels B, Wegscheider E, Hamel CP, Drexler W, Preising MN. Lack of fundus autofluorescence to 488 nanometers from childhood on in patients with early-onset severe retinal dystrophy associated with mutations in RPE65. *Ophthalmology*. 2004;111:1585–1594.
15. Paunescu K, Wabbels B, Preising MN, Lorenz B. Longitudinal and cross-sectional study of patients with early-onset severe retinal dystrophy associated with RPE65 mutations. *Graefes Arch Clin Exp Ophthalmol*. 2005;243:417–426.
16. Jacobson SG, Aleman TS, Cideciyan AV, et al. Defining the residual vision in Leber congenital amaurosis caused by RPE65 mutations. *Invest Ophthalmol Vis Sci*. 2009;50:2368–2375.
17. Hull S, Holder GE, Robson AG, et al. Preserved visual function in retinal dystrophy due to hypomorphic RPE65 mutations. *Br J Ophthalmol*. 2016;100:1499–1505.
18. Gu SM, Thompson DA, Srikumari CR, et al. Mutations in RPE65 cause autosomal recessive childhood-onset severe retinal dystrophy. *Nat Genet*. 1997;17:194–197.
19. Al-Khayer K, Hagstrom S, Pauer G, Zegarra H, Sears J, Traboulsi EI. Thirty-year follow-up of a patient with Leber congenital amaurosis and novel RPE65 mutations. *Am J Ophthalmol*. 2004;137:375–377.
20. Poehner WJ, Fossarello M, Rapoport AL, et al. A homozygous deletion in RPE65 in a small Sardinian family with autosomal recessive retinal dystrophy. *Mol Vis*. 2000;6:192–198.
21. Hamel CP, Griffoin JM, Lasquelléc L, Bazalgette C, Arnaud B. Retinal dystrophies caused by mutations in RPE65: assessment of visual functions. *Br J Ophthalmol*. 2001;85:424–427.
22. Magliyah M, Saifaldeen AA, Schatz P. Late presentation of RPE65 retinopathy in three siblings. *Doc Ophthalmol*. 2020;140:289–297.
23. Simovich MJ, Miller B, Ezzeldin H, et al. Four novel mutations in the RPE65 gene in patients with Leber congenital amaurosis. *Hum Mutat*. 2001;18:164.
24. Marlhens F, Bareil C, Griffoin JM, et al. Mutations in RPE65 cause Leber's congenital amaurosis. *Nat Genet*. 1997;17:139–141.
25. Marlhens F, Griffoin JM, Bareil C, Arnaud B, Claustres M, Hamel CP. Autosomal recessive retinal dystrophy associated with two novel mutations in the RPE65 gene. *Eur J Hum Genet*. 1998;6:527–531.
26. Kumaran N, Georgiou M, Bainbridge JWB, et al. Retinal Structure in RPE65-Associated Retinal Dystrophy. *Invest Ophthalmol Vis Sci*. 2020;61:47.
27. Simonelli F, Ziviello C, Testa F, et al. Clinical and molecular genetics of Leber's congenital amaurosis: a multicenter study of Italian patients. *Invest Ophthalmol Vis Sci*. 2007;48:4284–4290.
28. Sitorus RS, Lorenz B, Preising MN. Analysis of three genes in Leber congenital amaurosis in Indonesian patients. *Vision Research*. 2003;43:3087–3093.
29. Biswas P, Duncan JL, Maranhao B, et al. Genetic analysis of 10 pedigrees with inherited retinal degeneration by exome sequencing and phenotype-genotype association. *Physiol Genomics*. 2017;49:216–229.
30. Verma A, Perumalsamy V, Shetty S, Kulm M, Sundaresan P. Mutational screening of LCA genes emphasizing RPE65 in South Indian cohort of patients. *PLoS One*. 2013;8:e73172.
31. Srilekha S, Arokiasamy T, Srikrupa NN, et al. Homozygosity mapping in Leber congenital amaurosis and autosomal recessive retinitis pigmentosa in South Indian families. *PLoS One*. 2015;10:e0131679.
32. Singh HP, Jalali S, Narayanan R, Kannabiran C. Genetic analysis of Indian families with autosomal recessive retinitis pigmentosa by homozygosity screening. *Invest Ophthalmol Vis Sci*. 2009;50:4065–4071.
33. Hanein S, Perrault I, Gerber S, et al. Leber congenital amaurosis: comprehensive survey of the genetic heterogeneity, refinement of the clinical definition, and genotype-phenotype correlations as a strategy for molecular diagnosis. *Hum Mutat*. 2004;23:306–317.
34. Xu K, Xie Y, Sun T, Zhang X, Chen C, Li Y. Genetic and clinical findings in a Chinese cohort with Leber congenital amaurosis and early onset severe retinal dystrophy. *Br J Ophthalmol*. 2020;104:932–937.
35. Huang XF, Huang F, Wu KC, et al. Genotype-phenotype correlation and mutation spectrum in a large cohort of patients with inherited retinal dystrophy revealed by next-generation sequencing. *Genet Med*. 2015;17:271–278.
36. Colombo L, Maltese PE, Castori M, et al. Molecular epidemiology in 591 Italian probands with nonsyndromic retinitis pigmentosa and usher syndrome. *Invest Ophthalmol Vis Sci*. 2021;62:13.
37. Coppieters F, Casteels I, Meire F, et al. Genetic screening of LCA in Belgium: predominance of CEP290 and identification of potential modifier alleles in AHI1 of CEP290-related phenotypes. *Hum Mutat*. 2010;31:E1709–E1766.
38. Wiszniewski W, Lewis RA, Stockton DW, et al. Potential involvement of more than one locus in trait manifestation for individuals with Leber congenital amaurosis. *Hum Genet*. 2011;129:319–327.
39. Kondo H, Qin M, Mizota A, et al. A homozygosity-based search for mutations in patients with autosomal recessive retinitis pigmentosa, using microsatellite markers. *Invest Ophthalmol Vis Sci*. 2004;45:4433–4439.
40. Wang H, Wang X, Zou X, et al. Comprehensive molecular diagnosis of a large Chinese Leber congenital amaurosis cohort. *Invest Ophthalmol Vis Sci*. 2015;56:3642–3655.
41. Zernant J, Kulm M, Dharmaraj S, et al. Genotyping microarray (disease chip) for Leber congenital amaurosis: detection of modifier alleles. *Invest Ophthalmol Vis Sci*. 2005;46:3052–3059.
42. Chung DC, Bertelsen M, Lorenz B, et al. The natural history of inherited retinal dystrophy due to biallelic mutations in the RPE65 gene. *Am J Ophthalmol*. 2019;199:58–70.
43. Pierrache LHM, Ghafaryasl B, Khan MI, et al. Longitudinal study of Rpe65-associated inherited retinal degenerations. *Retina*. 2020;40:1812–1828.
44. Gao FJ, Wang DD, Li JK, et al. Frequency and phenotypic characteristics of RPE65 mutations in the Chinese population. *Orphanet J Rare Dis*. 2021;16:174.
45. Karcic S, Azzolini C, Alikadic-Husovic A. Telemedicine in vitreoretinal surgery. *Med Arh*. 1999;53:73–75.
46. Kalhori SRN, Hemmat M, Noori T, Heydarian S, Katigari MR. Quality evaluation of English mobile applications for gestational diabetes: app review using Mobile Application Rating Scale (MARS). *Curr Diabetes Rev*. 2021;17:161–168.

47. Makhni MC, Riew GJ, Sumathipala MG. Telemedicine in orthopaedic surgery: challenges and opportunities. *J Bone Joint Surg Am.* 2020;102:1109–1115.
48. Azzolini C. A pilot teleconsultation network for retinal diseases in ophthalmology. *J Telemed Telecare.* 2011;17:20–24.
49. Azzolini C, Torreggiani A, Eandi C, et al. A teleconsultation network improves the efficacy of anti-VEGF therapy in retinal diseases. *J Telemed Telecare.* 2013;19:437–442.
50. Azzolini C, Congiu T, Donati S, et al. Multilayer microstructure of idiopathic epiretinal macular membranes. *Eur J Ophthalmol.* 2017;27:762–768.
51. Donati S, Gandolfi C, Caprani SM, Cattaneo J, Premoli L, Azzolini C. Evaluation of the effectiveness of treatment with dexamethasone intravitreal implant in cystoid macular edema secondary to retinal vein occlusion. *BioMed Res Int.* 2018;2018:3095961.
52. Donati S, Maresca AM, Cattaneo J, et al. Optical coherence tomography angiography and arterial hypertension: A role in identifying subclinical microvascular damage? *Eur J Ophthalmol.* 2021;31:158–165.
53. Azzolini C, Donati S, Premi E, et al. SARS-CoV-2 on ocular surfaces in a cohort of patients with COVID-19 from the Lombardy Region, Italy. *JAMA Ophthalmol.* 2021;139:956–963.
54. Holladay JT. Visual acuity measurements. *J Cataract Refract Surg.* 2004;30:287–290.
55. McCulloch DL, Marmor MF, Brigell MG, et al. ISCEV Standard for full-field clinical electroretinography (2015 update). *Doc Ophthalmol.* 2015;130:1–12.
56. Han IC, Jaffe GJ. Comparison of spectral- and time-domain optical coherence tomography for retinal thickness measurements in healthy and diseased eyes. *Am J Ophthalmol.* 2009;147:847–858, 858 e841.
57. Kong X, Strauss RW, Michaelides M, et al. Visual Acuity Loss and Associated Risk Factors in the Retrospective Progression of Stargardt Disease Study (ProgStar Report No. 2). *Ophthalmology.* 2016;123:1887–1897.
58. Testa F, Melillo P, Bonnet C, et al. Clinical Presentation and Disease Course of Usher Syndrome Because of Mutations in Myo7a or Ush2a. *Retina.* 2017;37:1581–1590.
59. Glynn RJ, Rosner B. Regression methods when the eye is the unit of analysis. *Ophthalmic Epidemiol.* 2012;19:159–165.
60. Kopanos C, Tsiolkas V, Kouris A, et al. VarSome: the human genomic variant search engine. *Bioinformatics.* 2019;35:1978–1980.
61. Richards S, Aziz N, Bale S, et al. Standards and guidelines for the interpretation of sequence variants: a joint consensus recommendation of the American College of Medical Genetics and Genomics and the Association for Molecular Pathology. *Genet Med.* 2015;17:405–424.
62. Morimura H, Fishman GA, Grover SA, Fulton AB, Berson EL, Dryja TP. Mutations in the RPE65 gene in patients with autosomal recessive retinitis pigmentosa or Leber congenital amaurosis. *Proc Natl Acad Sci U S A.* 1998;95:3088–3093.
63. Perrault I, Rozet JM, Ghazi I, et al. Different functional outcome of RetGC1 and RPE65 gene mutations in Leber congenital amaurosis. *Am J Hum Genet.* 1999;64:1225–1228.
64. Lotery AJ, Namperumalsamy P, Jacobson SG, et al. Mutation analysis of 3 genes in patients with Leber congenital amaurosis. *Arch Ophthalmol.* 2000;118:538–543.
65. Astuti GD, Bertelsen M, Preising MN, et al. Comprehensive genotyping reveals RPE65 as the most frequently mutated gene in Leber congenital amaurosis in Denmark. *Eur J Hum Genet.* 2016;24:1071–1079.
66. Thompson DA, Gyurus P, Fleischer LL, et al. Genetics and phenotypes of RPE65 mutations in inherited retinal degeneration. *Invest Ophthalmol Vis Sci.* 2000;41:4293–4299.
67. Cideciyan AV. Leber congenital amaurosis due to RPE65 mutations and its treatment with gene therapy. *Progress in Retinal and Eye Research.* 2010;29:398–427.
68. Gardiner KL, Cideciyan AV, Swider M, et al. Long-Term structural outcomes of late-stage RPE65 gene therapy. *Mol Ther.* 2020;28:266–278.
69. Maguire AM, Bennett J, Aleman EM, Leroy BP, Aleman TS. Clinical Perspective: Treating RPE65-Associated Retinal Dystrophy. *Mol Ther.* 2021;29:442–463.
70. Jakobsson C, Othman IS, Munier FL, Schorderet DF, Abouzeid H. Cone-rod dystrophy caused by a novel homozygous RPE65 mutation in Leber congenital amaurosis. *Klin Monbl Augenbeilkd.* 2014;231:405–410.
71. Sodi A, Banfi S, Testa F, et al. RPE65-associated inherited retinal diseases: consensus recommendations for eligibility to gene therapy. *Orphanet J Rare Dis.* 2021;16:257.
72. Maguire AM, High KA, Auricchio A, et al. Age-dependent effects of RPE65 gene therapy for Leber's congenital amaurosis: a phase 1 dose-escalation trial. *Lancet.* 2009;374:1597–1605.
73. Avila-Fernandez A, Cantalapiebra D, Aller E, et al. Mutation analysis of 272 Spanish families affected by autosomal recessive retinitis pigmentosa using a genotyping microarray. *Mol Vis.* 2010;16:2550–2558.
74. Pasadhika S, Fishman GA, Stone EM, et al. Differential macular morphology in patients with RPE65-, CEP290-, GUCY2D-, and AIPL1-related Leber congenital amaurosis. *Invest Ophthalmol Vis Sci.* 2010;51:2608–2614.
75. Samardzija M, von Lintig J, Tanimoto N, et al. R91W mutation in Rpe65 leads to milder early-onset retinal dystrophy due to the generation of low levels of 11-cis-retinal. *Hum Mol Genet.* 2008;17:281–292.
76. Kumaran N, Rubin GS, Kalitzeos A, et al. A cross-sectional and longitudinal study of retinal sensitivity in RPE65-associated leber congenital amaurosis. *Invest Ophthalmol Vis Sci.* 2018;59:3330–3339.
77. Russell S, Bennett J, Wellman JA, et al. Efficacy and safety of voretigene neparvovec (AAV2-hRPE65v2) in patients with RPE65-mediated inherited retinal dystrophy: a randomised, controlled, open-label, phase 3 trial. *Lancet.* 2017;390:849–860.
78. Lopez-Rodriguez R, Lantero E, Blanco-Kelly F, et al. RPE65-related retinal dystrophy: mutational and phenotypic spectrum in 45 affected patients. *Exp Eye Res.* 2021;212:108761.
79. Le Meur G, Lebranchu P, Billaud F, et al. Safety and Long-Term Efficacy of AAV4 Gene Therapy in Patients with RPE65 Leber Congenital Amaurosis. *Mol Ther.* 2018;26:256–268.
80. Testa F, Melillo P, Della Corte M, et al. Voretigene-neparvovec gene therapy in clinical practice: treatment of the first two Italian pediatric patients. *Transl Vis Sci Technol.* 2021;10(10):11.